Available online at www.sciencedirect.com
ScienceDirect
Bioorganic & Medicinal Chemistry Letters 18 (2008) 324–328
Bioorganic & Medicinal Chemistry Letters

Biphenyl amide p38 kinase inhibitors 2: Optimisation and SAR

Richard M. Angell,[†] Tony D. Angell, Paul Bamborough,[*] David Brown, Murray Brown, Jacky B. Buckton, Stuart G. Cockerill,[†] Chris D. Edwards, Katherine L. Jones, Tim Longstaff, Penny A. Smee, Kathryn J. Smith, Don O. Somers, Ann L. Walker and Malcolm Willson[‡]

GlaxoSmithKline R&D, Medicines Research Centre, Gunnels Wood Road, Stevenage, Hertfordshire SG1 2NY, UK

Received 8 August 2007; revised 10 October 2007; accepted 13 October 2007
Available online 17 October 2007

Abstract—The biphenyl amides are a novel series of p38 MAP kinase inhibitors. Structure–activity relationships of the series against p38α are discussed with reference to the X-ray crystal structure of an example. The series was optimised rapidly to a compound showing oral activity in an in vivo disease model.
© 2007 Elsevier Ltd. All rights reserved.

The biphenyl amides (BPAs) are a novel series of p38α/β MAP kinase inhibitors discovered through structure-based focused screening. As described elsewhere, crystallography was used to elucidate the binding mode of **1** and **3**.[1] This suggested that the part of the molecule that could be most readily varied was the cyanophenyl amide group, which lies in the outer lipophilic region of the ATP-binding site and points out towards solvent (Fig. 1). Array technology allowed a wide range of substituents to be introduced at this position using amide coupling.

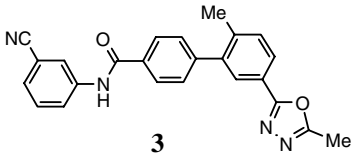

3

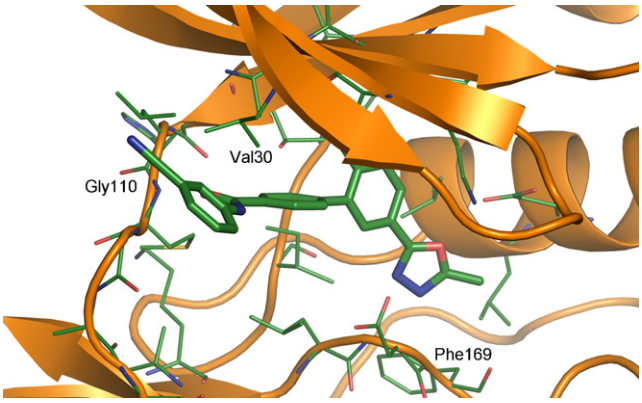

Figure 1. X-ray complex of p38α with **3**, focusing on the amide portion.

Compounds in Table 1 were prepared by a variety of similar routes. In the synthesis of **4** (Scheme 1), 3-bromo-4-methylbenzoic acid **A** was activated using CDI and coupled with *tert*-butylcarbazate to give the BOC-protected amide **B**. The BOC-group was removed using TFA to give the hydrazide **C**, which was refluxed with triethyl orthoacetate to form the 1,3,4-oxadiazole **D**. A Suzuki reaction with 4-carboxyphenylboronic acid under standard conditions produced **16** in good yield. The acid was converted to the acid chloride **E** using oxalyl chloride and then stirred with p-anisidine to give **4**.

Selected compounds illustrating SAR trends will now be discussed. Table 1 shows the p38α activity for a

Keywords: p38 kinase; p38α; p38; CSBP; MAP kinase; Inhibitors; BPA, biphenyl amide; BPAs, biphenyl amides; Protein kinase X-ray structure; Binding mode; Structure-based drug design; Kinase selectivity.
* Corresponding author. Tel.: +44 1438 763246; fax: +44 1438 763352; e-mail: paul.a.bamborough@gsk.com
† Present address: Arrow Therapeutics, Britannia House, 7 Trinity Street, London SE1 1DA, UK.
‡ Present address: Genomic Solutions, 1B Blackstone Road, Huntingdon, Cambridgeshire PE29 6EF, UK.

0960-894X/$ - see front matter © 2007 Elsevier Ltd. All rights reserved.
doi:10.1016/j.bmcl.2007.10.043

Table 1. Activity of selected phenyl and benzyl amide analogues against p38α (μM)[2]

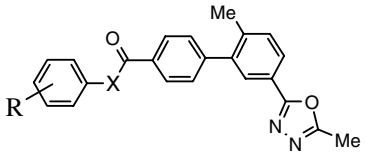

Compound	X	R	IC_{50}	K_i
1	NH	3-(4-Me piperazine), 4-OMe	10	1.6
2	NH	3-(4-Me piperazine)	3.1	0.49
3	NH	3-CN	1.5	0.24
4	NH	4-OMe	2.3	0.36
5	NH	2-OMe	1.6	0.25
6	NH	3-CONHMe	0.60	0.10
7	NH	4-$NHSO_2Me$	0.28	0.04
8	$NHCH_2$	4-$NHSO_2Me$	0.28	0.04
9	$NHCH_2$	4-H	0.61	0.10
10	$NHCH_2$	3-OMe	0.37	0.06
11	$NHCH_2$	4-OMe	0.52	0.08
12	$NHCH_2$	4-Cl	0.60	0.10
13	$NHCH_2$	3-(Methylmorpholine)	0.87	0.14
14	$N(Me)CH_2$	4-Cl	0.89	0.14
15	NMe	3-CN	12	1.9

variety of phenyl and benzyl amide substituents. The data shown are from a binding assay measuring the displacement of a fluorescent ATP-competitive ligand.[2]

Removing the methoxy from the phenylpiperazine ring of **1** to give **2** increases potency, perhaps because it allows the phenylpiperazine rings to adopt a more planar conformation. The piperazine ring is not required for p38α potency (**3**,**4**). The outer aromatic ring makes lipophilic interactions with Val30, but is accessible to solvent, so the expectation was that there would be only small substituent effects on the potency. Electron-withdrawing and donating groups, as well as larger meta and para substituents, are tolerated without loss of activity (**3**–**7**). Modelling from the X-ray structure of **3** offers no explanation for the increased affinity of **7**.

Apart from phenyl-substituted amides, the best enzyme activity comes from compounds bearing benzyl amides (compounds **8**–**13**). As with phenyl amides, the substitution pattern does not greatly change the activity. Benzyl amides are comparable to or better than the corresponding phenyl amides (for example **4** and **11**, **7** and **8**). Even bulky 4-substituents on the benzylic ring are well tolerated (**13**). These groups presumably pass beyond Val30 towards solvent.

Further substitution on the benzylic amide nitrogen with *N*-methyl does not lead to a significant loss of potency (compare **14** and **12**). This is consistent with the environment of the amide NH in the X-ray structure of **3**. No protein atom or visible water lies close enough to prevent substitution. However, N-substitution on phenyl amides causes a greater loss of activity (compare **15** and **3**). This can be attributed to intramolecular steric interactions between the amide methyl group and both of the adjacent phenyl rings, destabilising the bound conformation.

Various flexible groups were introduced at the amide position, intended to project into solvent and to improve solubility. In contrast to aromatic substituents, small or flexible substituents have greatly reduced potency (Table 2, **17**–**20**). The precursor acid **16** shows only very weak activity, while the cyclopropylmethyl **17** is the most potent alkyl amide. This reinforces the need for lipophilic amide substituents to interact with the 'outer lipophilic

Table 2. p38α activity of selected amide analogues (μM)[2]

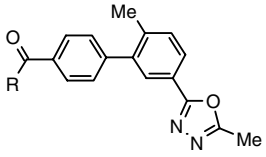

Compound	R	IC_{50}	K_i
16	OH	>16	>2.5
17	$NH(CH_2)$-cyclopropyl	3.0	0.48
18	$NH(CH_2)_3OH$	7.1	1.1
19	$NH(CH_2)_2$-morpholine	>16	>2.5
20	1-Piperidine	10	1.6

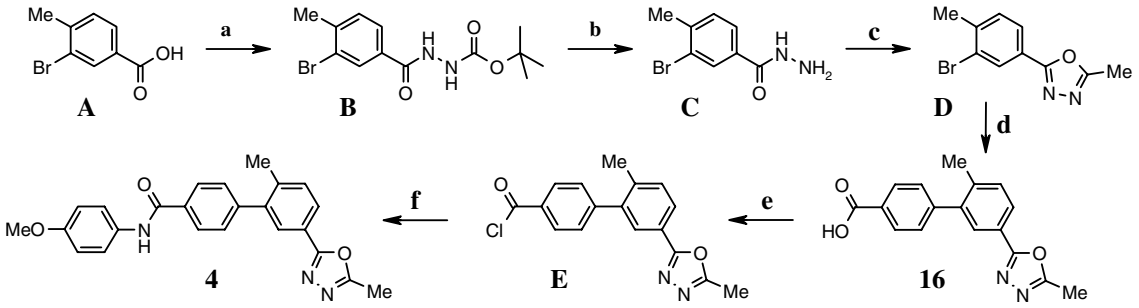

Scheme 1. Reagents and conditions: (a) CDI, *tert*-butylcarbazate, THF 48%; (b) TFA, 56%; (c) triethyl orthoacetate, 155 °C, 86%; (d) 4-carboxyphenylboronic acid, $Pd(PPh_3)_4$, 2 M sodium carbonate (aq), DME, 91%; (e) oxalyl chloride, DCM, DMF, 100%; (f) p-anisidine, triethylamine, THF.

pocket' of the ATP site (Val30 or Ala111). Straight-chain alkyl alcohols (e.g., **18**) are tolerated, but with lowered activity. The flexibility of this group may incur a penalty due to loss of entropy on binding. Basic chains including those containing tertiary amines suffer a greater loss of activity (e.g., **19**). Cyclisation incorporating the amide nitrogen is also unfavourable (e.g., **20**).

Having explored SAR at the amide position, the next changes concentrated on replacing the oxadiazole ring. The activities of **21**–**29** are given in Table 3. The 1,3,4-oxadiazoles (**21**–**24**) were synthesised as in Scheme 1, using different orthoesters at step (c) to vary the substitution in the 5-position. Synthesis of the 1,2,4-oxadiazole (**25**) was achieved by oxadiazole formation from the acid followed by a Suzuki reaction to form the biaryl ring system (Scheme 2). **26** was synthesised by forming the pinacolatoborane on the biaryl core and reacting with 2-bromo-1*H*-imidazole under Suzuki conditions (Scheme 3). Reaction of **17** with benzylamine under microwave conditions gave the benzyl protected 1,3,4-triazole which was hydrogenated to **27** (Scheme 4).

Table 3. p38α activity (μM) of selected modifications to the biphenyl-1,3,4-oxadiazole[2]

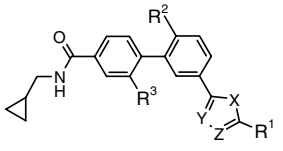

Compound	X	Y	Z	R^1	R^2	R^3	IC_{50}	K_i
17	O	N	N	Me	Me	H	3.0	0.48
21	O	N	N	H	Me	H	>16	>2.5
22	O	N	N	Et	Me	H	10	1.6
23	O	N	N	Pr	Me	H	9.7	1.5
24	O	N	N	Bu	Me	H	>16	>2.5
25	N	N	O	Me	Me	H	14	2
26	N	N	C	H	Me	H	11	1.7
27	N	N	N	Me	Me	H	1.4	0.22
28	O	N	N	Me	H	H	>16	>2.5
29	O	N	N	Me	H	Me	>16	>2.5

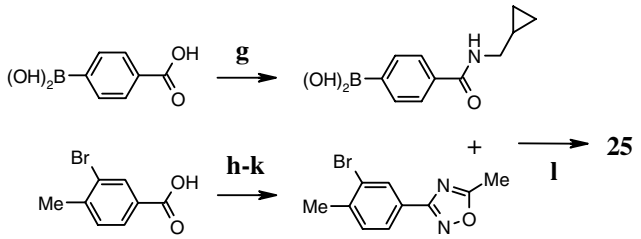

Scheme 2. Reagents and conditions: (g) i—HBTU, HOBT, DIPEA, DMF; ii—cyclopropyl methylamine, 40%; (h) i—oxalyl chloride, DCM, DMF; ii—0.5 M NH_3 in dioxane, 83%; (i) TFAA, pyridine, DCM, 65%; (j) hydroxylamine hydrochloride, 80 °C, 73%; (k) NaOMe in MeOH, acetic anhydride, DMF, 50 °C, 41%; (l) $Pd(PPh_3)_4$, Cs_2CO_3, DMF, 90 °C, 24%.

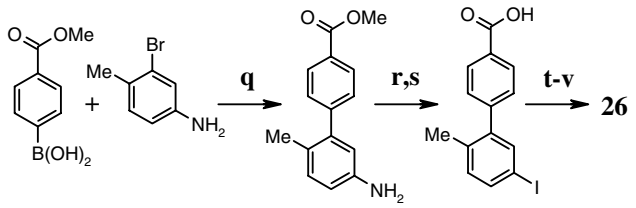

Scheme 3. Reagents and conditions: (q) $Pd(PPh_3)_4$, Cs_2CO_3, ethyleneglycol–dimethylether, 90 °C, 50%; (r) $NaNO_2$, KI, 5 M HCl (aq), 0–60 °C, 30%; (s) 2 M NaOH (aq), MeOH, 89%; (t) i—thionyl chloride, reflux; ii—cyclopropylmethyl amine, Na_2CO_3, DCM, 41%; (u) i—bis(pinacolato)diboron, KOAc, $PdCl_2(dppf)$, DMF, 80 °C, 74%; (v) i—2-bromo-1*H*-imidazole, $Pd(PPh_3)_4$, 2 M Na_2CO_3 (aq), DMF; ii—$PdCl_2(dppf)$, 100 °C, 5%.

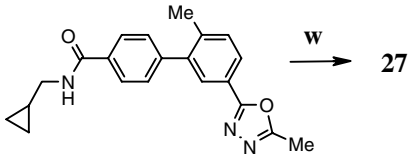

Scheme 4. Reagents: (w) i—Benzylamine, NMP, microwave; ii—10% Pd/C, formic acid, ethanol, 27%.

Compound **28** was prepared by a similar route to Scheme 1 using 3-bromobenzoic acid instead of **A**. **29** was prepared as shown in Scheme 5.

In the X-ray structure of **3** (Fig. 2), the methyl on the oxadiazole (R^1 in Table 3) fits snugly into a small lipophilic pocket close to Leu171. Replacing this methyl with hydrogen (**21**) results in a loss in activity of at least fivefold relative to **17**. Groups such as ethyl, propyl and butyl (**22**–**24**), which modelling suggests are too large to fit in this pocket without clashing with Leu171, show reduced activity with increasing size.

The nitrogen atoms of the 1,3,4-oxadiazole are within hydrogen-bonding distance of the backbone NH atoms of Asp168 and Phe169 (Fig. 2). The oxadiazole oxygen is close to the sidechain oxygen of Glu71, an unfavourable position for an electronegative atom. It was expected that exchanging other heterocycles for the oxadiazole would change these interactions and hence the potency. The 1,2,4-oxadiazole (**25**) is less potent than **17** by a factor of nearly 5. Two factors can explain this. First, aromatic oxygen atoms are poor hydrogen-bond acceptors. The alternative isomer would replace a strong H-bond from aromatic nitrogen to Phe169 with a weak one from aromatic oxygen. In addition, the 1,2,4-oxadiazole would place nitrogen, a more electronegative atom than oxygen, close to the acid sidechain of Glu71.

Other heterocycles were prepared, for example the imidazole **26**, but all are weaker inhibitors than the 1,3,4-oxadiazole with the exception of the 1,3,4-triazole (**27**). The triazole tautomer with the hydrogen at the N4 position (Fig. 3) would be able to donate a hydrogen-bond to Glu71 while retaining both H-bond acceptor functionalities of the 1,3,4-oxadiazole. However, the twofold

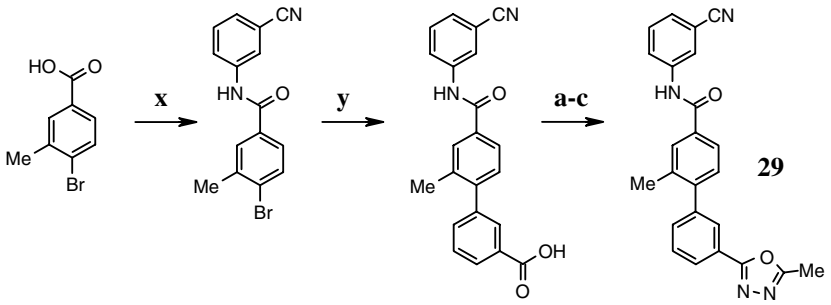

Scheme 5. Reagents and conditions: (x) i—$SOCl_2$; reflux 2 h; ii—3-aminobenzonitrile, triethylamine, THF, 76%; (y) 3-(dihydroxyboranyl)benzoic acid, Pd(PPh3)4, 2 M sodium carbonate (aq), DME, 60%. Steps (a–c) are as in Scheme 1.

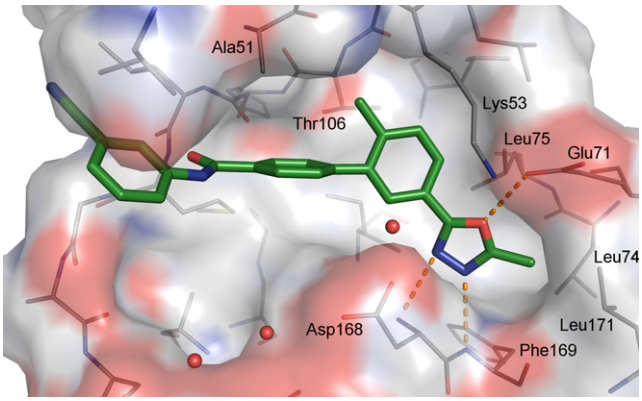

Figure 2. X-ray complex of **3** highlighting the oxadiazole interactions.

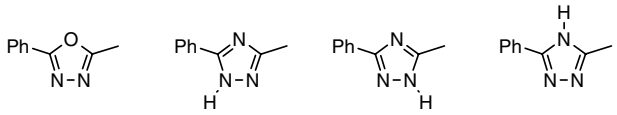

Figure 3. Oxadiazole vs triazole tautomers for a model system.

gain in potency is modest, perhaps because in gas-phase calculations this N4-H tautomer is significantly higher in energy than N2-H.[3]

The toluene methyl adjacent to the biaryl bond fills a small pocket between Ala51 and Thr106.[1] **28** (R^2 = H) was made to investigate the importance of this and was very weakly active. This shows the need either to fill this small pocket, or for the biphenyl to adopt a perpendicular arrangement, for activity. The low activity of **29**, where the methyl was moved onto the adjacent phenyl ring, suggests that the former is the most important factor.

Compounds from the BPA series were highly selective. **17** was tested in 38 other in vitro protein kinase assays, including CDK2, GSK-3β, JNK isoforms 1–3, Lck, ROCK1 and VEGFR2, while **10** was tested in 24 assays. Both compounds bind to p38β with similar affinity to p38α, with IC_{50} of 0.7 μM (K_i 0.16 μM) for **10** and IC_{50} of 1.8 μM (K_i 0.44 μM) for **17**. No other kinase was inhibited with IC_{50} below 16 μM, so **10** shows at least 40-fold selectivity in IC_{50} against all kinases tested.

Compounds were assayed for their ability to inhibit the production of TNFα in LPS-stimulated peripheral blood mononuclear cells.[4] **1** did not reproducibly show activity in this assay at the concentration range tested. Compounds which were more potent in the enzyme assay showed much improved dose–response curves in PBMCs. For example, **17** has an IC_{50} of 2.5 μM (mean of 10 values, standard deviation 0.88).

In addition, **17** shows an excellent pharmacokinetic profile in the rat, displaying good oral bioavailability, a low plasma clearance, moderate volume of distribution and a long plasma half-life (Table 4).[5]

17 was tested in a rat model of acute joint inflammation.[6] The PG–PS (Streptococcal cell wall) reactivation arthritis model has been shown to be particularly sensitive to inhibitors of TNFα and IL-1, and is therefore a suitable model for testing compounds which affect the

Table 4. Pharmacokinetic parameters of **17** measured in rat[5]

IV plasma clearance (ml/min/kg)	<10
IV steady state volume of distribution (l/kg)	2
IV plasma terminal $t_{1/2}$ (h)	9–13
Oral bioavailability	50%

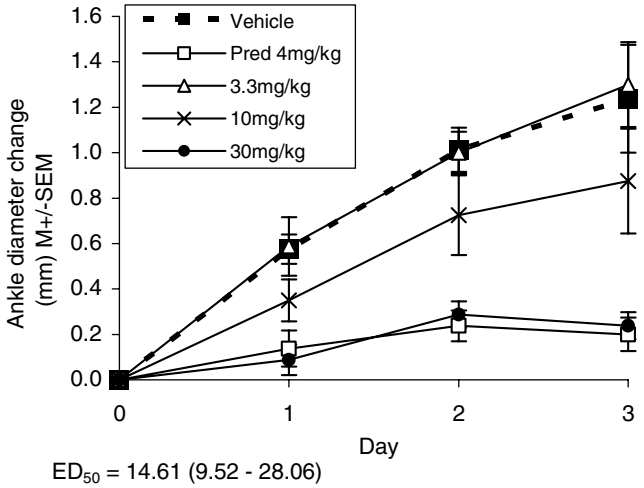

Figure 4. Dose-dependent inhibition of ankle swelling in the rat PGPS model.[6]

synthesis and activity of pro-inflammatory cytokines. The compound shows dose-dependent anti-inflammatory activity with an ED_{50} of 15 mg/kg. Figure 4 shows results for dosing **17** at 3.3, 10 and 30 mg/kg. Also shown are results for the vehicle and prednisolone at 4 mg/kg. At 30 mg/kg, activity is comparable to that of 4 mg/kg prednisolone.

The in vivo activity is very encouraging for this new template, especially considering its modest enzyme potency. Furthermore, given the selective kinase inhibition profile of this compound, it is likely that the in vivo activity is driven by inhibition of p38.

In summary, compound **17** shows significant progress over compound **1**. It is a potent, selective inhibitor of p38α with cellular activity, oral bioavailability and activity in an in vivo model of joint inflammation. Future publications will describe the continuing development of the biphenyl amide series.

Acknowledgment

The authors thank Rick Williamson for suggestions and for contributing experimental details.

References and notes

1. Angell, R. M.; Bamborough, P.; Cleasby, A.; Cockerill, S. G.; Jones, K. L.; Mooney, C. J.; Somers, D. O.; Walker, A. L. *Bioorg. Med. Chem. Lett.* **2008**, *18*, 318.
2. (a) Fluorescence polarisation assays used GST-tagged p38α (activated using MKK6 and re-purified) or GST-tagged truncated JNK3 (residues 39–402) and an ATP-competitive rhodamine-green labelled fluoroligand (2-(6-amino-3-imino-3H-xanthen-9-yl)-5-{[({4-[4-(4-Cl-3-hydroxyphenyl)-5-(4-pyridinyl)-1*H*-imidazol-2yl]phenyl}methyl)amino]carbonyl}benzoic acid). These components were dissolved in a buffer of final composition 62.5 mM Hepes, pH 7.5, 1.25 mM CHAPS, 1 mM DTT, 12.5 mM $MgCl_2$, with final concentrations of 12 nM of p38α or 50 nM JNK3 and 5 nM fluoroligand. Thirty microliters of this mixture were added to wells containing 1 μl of test compound (0.28 nM–16.6 μM) and incubated for 30–60 min at room temperature. Fluorescence anisotropy was read in a Molecular Devices Acquest (excitation 485 nm/emission 535 nm); (b) The Cheng–Prusoff equation (Cheng, Y.-C.; Prusoff, W. H. *Biochem. Pharmacol.* **1973**, *22*, 3099–3108), $K_i = IC_{50}*(1+([S]/K_m))$, was used to calculate K_i from determined IC_{50} for activity assays. To calculate K_i from determined IC_{50} for fluorescence polarisation assays a modification of the Cheng–Prusoff equation was used (Cheng, H. C. *Pharmacol. Res.* **2005**, *50*, 21–40). $K_i = IC_{50}*(1+((n[E])/K_d))$ where n is the fraction of enzyme competent to bind fluoroligand. K_i values for 381 compounds in the fluorescence polarisation assay correlate with those from an activity assay (details to be published) with $r^2 = 0.9$.
3. Gas-phase optimisation of the three phenyltriazole tautomers in the model compound 3-methyl-5-phenyl-1*H*-1,2,4-triazole was performed using B3LYP DFT with a 6-31g**+ basis set in JAGUAR v4.0; Schrödinger Inc.: Portland, OR, 2000. Triazole tautomer N4-H would be capable of donating the H-bond to Glu71, but its enthalpy of formation is 7.0 kcal/mol less stable than tautomer N2-H. Tautomer N1-H is only 0.4 kcal/mol less stable than N2-H.
4. Human peripheral blood mononuclear cells (PBMCs) were prepared from heparinised human blood from normal volunteers by centrifugation on hystopaque 1077 at 1000*g* for 30 min. The cells were collected from the interface, washed by centrifugation (1300*g*, 10 min) and re-suspended in assay buffer (RPMI1640 containing 10% foetal calf serum, 1% L-glutamine and 1% penicillin/streptomycin) at 1×10^6 cells/ml. Fifty microliter cells were added to microtitre wells containing 50 μl of an appropriately diluted compound solution (prepared from 10 mM stock in DMSO by serial dilution in assay buffer giving maximally 0.1% DMSO final). After 10–15 min incubation, lipopolysaccharide (s. typhosa, sigma) was added giving 1 ng/ml final concentration. The assay plates were incubated at 37 °C, 5% CO_2 for 18–20 h and cell free supernatants collected following centrifugation at 800*g*. The supernatant was then assayed for TNFα using a commercially available ELISA (Pharmingen).
5. Pharmacokinetic parameters in male Lewis rats were determined following intravenous (iv) and oral (po) administration at 1 and 3 mg/kg, respectively. Compound was administered as a solution in 20% DMSO: 80% PEG200 (iv) or 5% DMSO: 40% Vit E: 40% PEG400: 15% Mannitol (po). Blood was collected over a 24-h time period. Plasma was prepared following centrifugation and compound extracted from 50 μL plasma using protein precipitation with acetonitrile. Samples were then evaporated under nitrogen and re-suspended in 100 μl of 10:90 acetonitrile:water. Analysis was performed using LC–MSMS on the API365 with a 5 min fast gradient comprising 0.1% formic acid in water and 0.1% formic acid in acetonitrile (mobile phases), 20μl injection volume, flow rate 4 ml/min and ODS3 Prodigy column (5 cm × 2.1 mm, 5 μm). Pharmacokinetic data were generated using PKTools.
6. PG–PS (peptidoglycan–polysaccharide from Streptococcal cell walls) was injected intra-articularly and followed two weeks later by a systemic reactivation using the same bacterial cell wall component. The reactivated joint swelling was measured for 3 days after systemic challenge while dosing orally, twice daily, with the target compound.